IEEE Access
Multidisciplinary | Rapid Review | Open Access Journal

Received November 22, 2021, accepted December 6, 2021, date of publication January 11, 2022, date of current version February 18, 2022.

Digital Object Identifier 10.1109/ACCESS.2022.3142014

Field-Oriented Control of Five-Phase Induction Motor Fed From Space Vector Modulated Matrix Converter

KHALIQUR RAHMAN[1], SYED RAHMAN[2], (Student Member, IEEE), MAHAJAN SAGAR BHASKAR[3], (Senior Member, IEEE), ATIF IQBAL[4], (Senior Member, IEEE), AMITH KHANDAKAR[4], (Senior Member, IEEE), MOHD TARIQ[1], (Senior Member, IEEE), AND BASEM ALAMRI[5], (Member, IEEE)

[1]Department of Electrical Engineering, ZHCET, Aligarh Muslim University, Aligarh 202002, India
[2]Department of Electrical and Computer Engineering, Texas A&M University, College Station, TX 77843, USA
[3]Renewable Energy Laboratory, Department of Communications and Networks Engineering, College of Engineering, Prince Sultan University, Riyadh 12435, Saudi Arabia
[4]Department of Electrical Engineering, Qatar University, Doha, Qatar
[5]Department of Electrical Engineering, College of Engineering, Taif University, Taif 21944, Saudi Arabia

Corresponding authors: Mohd Tariq (tariq.ee@zhcet.ac.in) and Amith Khandakar (amitk@qu.edu.qa)

This work was supported in part by the Qatar National Research Fund under NPRP Grant 4-152-2-053; in part by the Taif University Researchers Supporting Project, Taif University, Taif, Saudi Arabia, under Grant TURSP-2020/278; and in part by the Collaborative Research Grant Scheme (CRGS) Project, Hardware-In-the-Loop (HIL) Laboratory, Department of Electrical Engineering, Aligarh Muslim University, India, under Project CRGS/MOHD TARIQ/01 and Project CRGS/MOHD TARIQ/02.

ABSTRACT This paper presents the field-oriented control (FOC) of a five-phase induction motor (FPIM) fed from a three-to-five phase direct matrix converter (DMC). The article focuses on the modulation and control of the three-to-five phase DMC, which discusses minimizing the problems associated with switching vector selection, sector identification, switching sequence selection, and dwell-time calculations. The DMC is controlled from the space vector pulse width modulation (SVPWM) technique, eliminating the x-y components of space vectors. Moreover, the matrix converter can perform unity power factor control at the input side. The FPIM is sourced from a DMC, and the FOC technique is applied to control the drive. The dynamic characteristics of the drive are succeeded for different loading conditions. The proposed work is simulated in Simulink/Matlab environment and further verified through practical experimentation. The control signals of the IGBTs are generated through FPGA embedded in dSPACE 1006. The experimental and the simulation results prove the practicability of the FOC to FPIM fed from a DMC.

INDEX TERMS Direct matrix converter, five-phase induction motor, field-oriented control, multiphase, space vector pulse width modulation.

I. INTRODUCTION

Easy availability, simple construction, cost-effectiveness, and ruggedness are the main reasons for the preference for three-phase drive systems. However, with the advances in power electronics, the number of phases of a drive system has also become a design parameter. From the literature, it is obtained that the multiphase offers additional advantages such as higher reliability, improved harmonic performance, precise control, higher torque density, and minimizing the effect of torque pulsations by shifting them further up on the frequency domain. Various works have shown that a multiphase drive system with a stator having a higher phase number enables smooth and independent vector control operation for speed control [1]–[4].

Performance factors such as dc bus utilization, switching losses, harmonic performance, etc., are decided by the modulation method of the converter in the drive system. There are two main categories of pulse width modulation methods available in the literature. For a three-phase motor drive, sine–triangle PWM (SPWM) is the simplest modulation method. However, the switching signal duty cycles are derived from the other PWM strategies, such as SVPWM. This method is categorized with higher dc bus utilization by achieving more

The associate editor coordinating the review of this manuscript and approving it for publication was Pinjia Zhang.

increased ac RMS output voltage (almost 15% higher than SPWM for three-phase) [5]–[7]. However, this limit is lower for multiphase operation and depends on the output voltage space vector components. In the five-phase SVPWM, the five voltages are converted through multiple d-q transformations to give main and auxiliary space vectors. Initial publications only focused on the realization of sinusoidal voltage generation. However, the effect of the additional space vector (x-y components) on the waveform quality is analyzed. Later methods are introduced to mitigate the auxiliary space vector effect while maximizing the impact of main space vectors [7].

Multiphase motors based electric drives for specialized applications have also become common in the last decade. Recently, an existing three-phase synchronous reluctance machine performance is compared with an identical machine that is upgraded to a five-phase machine. The performance parameters were torque ripple and torque, in fault and healthy conditions. The results verified that the five-phase had 11.8% higher torque, and after some modifications in the five-phase design, it had 17% lower torque ripple than the three-phase machine. Moreover, during a fault, the performance of multiphase was much better than three-phase [8]. Drive configurations commonly consist of back-to-back converters with an intermediate dc-link capacitor. However, this dc-link capacitor limits the system's reliability as these bulky capacitors have a short lifespan, deprived performance at a higher temperature, and are prone to dangerous failures.

Additionally, the dc-link capacitor also occupies a significant power board space to limit the power density. For addressing these concerns, direct ac-ac converters called matrix converters (MC) are introduced. A detailed discussion of two variants of MC, namely direct and indirect MC, is available in the literature [9], [10]. Matrix converters offer various benefits, including input power factor control, bidirectional power flow, higher power density, etc.

Indirect MC uses a lesser number of active switches and current sensors for realization. Indirect MC, when operated with a suitable modulation technique, eliminates the need for special commutation. However, non–linear modulation response and higher power losses are the problems associated with indirect MC. Several research outcomes have been described on multiphase MC modeling, control, and applications [11]–[15]. In SVPWM, instantaneous representation of output voltages and input currents are considered. SVPWM control technique provides complete control of both the input power factor and the output voltage.

Like conventional drive systems, MC-based FPIM drives also need to employ independent control of flux and torque of the motor to achieve a fast dynamic response. For traditional drives, direct torque and field-oriented control are two general methodologies for induction motor drives. The classical direct torque control (DTC) system requires only stator resistance information for their control [16]–[18]. However, DTC is a nonlinear control scheme that directly produces the voltage vectors without a modulator. FOC applied for induction motor uses PWM and linear controllers and has more popularity than DTC [19]–[22]. Many research work focusing on the FOC of FPIM supplied from a single voltage source-based two-level inverter are present. A detailed discussion of conventional FPIM based drive controlled with DTC and FOC is given in Table 1.

TABLE 1. General discussion of FOC versus DTC for conventional five phase induction motor performance.

Features	FOC	DTC [31]-[34]
Current THD [34]	Low (2.73%)	High (5.24%)
Tracking error	Very low	High
Torque ripple (4kHz)	6%	4.24%
Torque Dynamic	Fast	Very fast
Dynamic performance	Setting time (<0.5)	Setting time (<0.32 s)
	Rise time (~0.2 s)	Rise time (~ 0.11 s)
	Overshoot (~50%)	Overshoot ~20%
Coordinate ref. frame	d, q (stator)	α, β (stator)
Low speed behaviour (<5% of nominal)	Good with position or speed sensor	Required speed sensor for braking
Controlled variables	Rotor flux current i_d, torque current i_q vector components, rotor flux	Stator flux, torque and
Steady state distortion	Low	Low (high features current sensors requires)
Parameter sensitivity	Rotor resistance, d, q inductances,	d, q inductances, flux (near zero speed only)
Rotor position measurement	Required (either estimator or sensor)	Not required

The work done in the area of a multiphase systems powered by a matrix converter is very limited. Recently, a paper focuses on controlling a five-phase induction motor fed from a three-to-five phase matrix converter. The control is based on the direct torque control method, where, controlling the virtual vectors are controlled by selecting the active voltage vectors of the matrix converter [23]. Further, a case study has been presented in a research paper where it is obtained that there is possible to reduce the computational burden and precise control by using the model predictive control method. The virtual vectors control concept has been utilized to perform the model predictive direct torque control for a five-phase induction motor fed from a direct matrix converter [24].

Only a few FOC of three-phase matrix converter-based drive systems have been discussed in the existing literature [25]–[27]. Due to the deficiency of technical advancement, controlling multiphase induction motor fed from matrix converter is a significant issue. Therefore, this paper presents the field-oriented control of a five-phase drive fed from a three-to-five-phase matrix converter. Compared to a conventional three-phase system, in the case of FPIM, the additional xy components adversely impact the electromagnetic flux, thereby distorting the stator current. This research work proposes SVPWM based FOC method to eliminate this xy component by using the volt-sec balance technique to modulate active voltage vectors in a switching cycle [28], [29]. For this implementation, the paper presents a precise modulation of three-to-five phase DMC, which can solve the problems related to switching states, sector identification, switching sequence selection, and dwell-time calculations.

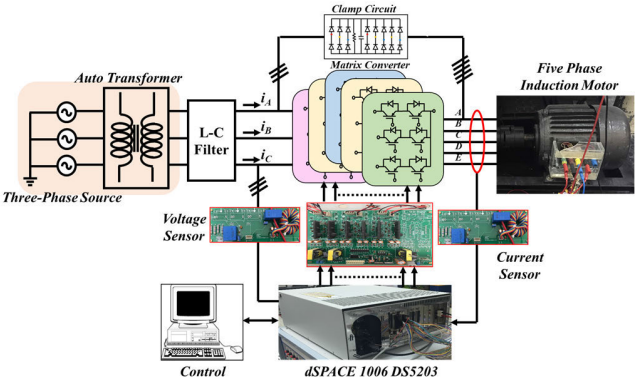

FIGURE 1. Configuration of the three-phase to five-phase DMC.

The effectiveness of the modulation strategy-based FOC of FPIM is validated using a laboratory prototype of 2-hp rated FPIM. Experimental results showing the elimination of xy component are also presented. The proposed method in an electric drive has been verified experimentally in the lab with a five-phase induction motor.

II. PROPOSED CONTROL SCHEME

The performance of the offered control technique is analyzed and discussed based on realistic numerical simulations of the whole drive system. Detailed configuration of the three-phase to five-phase DMC fed five phase induction motor system is shown in Fig. 1. Power from the three-phase source is fed to FPIM through DMC. For avoiding discontinuous current, a dedicated clamp circuit is placed in parallel with DMC.

The detailed FOC-based control algorithm is shown in Fig. 2. The induction motor speed is sensed and compared with the reference speed. The speed error is processed through a proportion integral (PI) controller to give the reference quadrature axis stator current I_{qsref}, which is further compared with actual I_{qs} obtained from the real currents of five phases. The stator's five-phase current is transformed into four orthogonally placed currents I_{ds}, I_{qs}, and I_x, I_y. The x-y currents component should be zero at a steady state. However, the error signal in I_{qs} is processed through the PI controller to give V_{qsref}.

Similarly, from the speed feedback, there is the look-up table for I_{mr}. In steady-state operation, I_{mr} will be equal to the I_{ds}. The I_{mr} is equated with the I_{ds}, and the difference will give V_{dsref} after passing through the PI controller. The obtained stator voltage reference generates the reference signal for the generation of switching pulses of the MC with the help of dq-to-ABCDE transformation. For this dq-to-five phase transformation, rho (ρ) is required. To obtain 'ρ' one has to go to the induction motor's actual speed and current. The motor currents are sensed and converted to $\alpha\beta$ and further to dq. The output of the transformed dq block gives I_{ds} (I_{mr}) and I_{qs} for feedback. The I_{mr} will be equal to the I_{mr_ref} in a steady-state; however, if any transient flux weakening is there, the correct I_{mr} becomes $I_{mr\_ref}/(1+sT_r)$. To compute the slip information from I_{qs} with the help of slip computational block, which gives slip speed in output. To find the synchronous speed, the slip speed is added with motor speed. Which further gives 'ρ' after the integration of speed. This 'ρ' can be needed in transformation blocks.

III. FOC IN THREE-TO-FIVE PHASE MATRIX CONVERTER FED FIVE-PHASE IM

The general equation for machine expressions can be written as (1). After the disturbance in the machine, one can get (2)-(3). Where V_0 is a point where the system was operating and ΔV is the disturbance in voltage.

$$V = RI + L_pI + G_1\omega_sI + G_2\omega_rI \tag{1}$$

$$V_0 + \Delta V = R(I_0 + \Delta I) + L_p(I_0 + \Delta I) + G_1(\omega_{s_0} + \Delta\omega_s) \times (I_0 + \Delta I) + G_2(\omega_{r_0} + \Delta\omega_r)(I_0 + \Delta I) \tag{2}$$

$$\Delta V = R\Delta I + L_p\Delta I + G_1\Delta\omega_sI_0 + G_1\omega_{s_0}\Delta I + G_2\omega_{r_0}\Delta I + G_2\Delta\omega_rI_0 \tag{3}$$

The torque can be written as (4), and to get the disturbing value of the torque, (6) is given.

$$T = I^TG_2I \tag{4}$$

$$T_0 + \Delta T = (I_0 + \Delta I)^TG_2(I_0 + \Delta I) \tag{5}$$

$$\Delta T = G_3\Delta I \tag{6}$$

The machines' mechanical equation can be written as,

$$J\frac{d\omega}{dt} = T - T_L - B\omega \tag{7}$$

$$Jp\Delta\omega_r = \Delta T - \Delta T_L - B\Delta\omega_r \tag{8}$$

Combining (3), (6), and (8), one can get state variable notation. Equation (9) is the state variable representation of the small vector. Here ΔI is a 4×1 vector if zero sequences are neglected. It should be ignored as there is no ground wire connected to the star of the stator neutrals.

$$P\begin{bmatrix}\Delta I\\ \Delta\omega\end{bmatrix} = \begin{bmatrix}L^{-1}(R + G_1\omega_{s0} + G_2\omega_{rs}) & -L^{-1}G_2I_0\\ \frac{G_3}{J} & \frac{-B}{J}\end{bmatrix} \times \begin{bmatrix}\Delta I\\ \omega_r\end{bmatrix} + \begin{bmatrix}L^{-1} & -L^{-1}G_1I_0 & 0\\ 0 & 0 & \frac{1}{J}\end{bmatrix}\begin{bmatrix}\Delta V\\ \Delta\omega_s\\ \Delta T_L\end{bmatrix} \tag{9}$$

By transforming in Laplace domain,

$$pX = Ax + Bu \tag{10}$$

$$sX(s) = Ax(s) + Bu(s) \tag{11}$$

$$X(s) = (sI - A)^{-1}Bu(s) \tag{12}$$

From (12), for any input 'u', we can find the response 'x'. α_s and β_s are the stator axis in the stationary reference frame and transform the equations in the synchronous reference frame shown by axis d_s and q_s in Fig. 3. The angle between α_s and d_s is rho (ρ) and its rate of change, i.e., synchronous speed. Neglecting zero-sequence voltage, d-axis stator voltage can be written as (13).

$$V_{ds} = (r_s + L_{ss}p)i_{ds} - \omega_sL_{ss}i_{qs} + L_mpi^{ds} - L_m\omega_si^{qs} \tag{13}$$

$$\psi_{ds} = L_{ss}i_{ds} + L_mi^{ds} \tag{14}$$

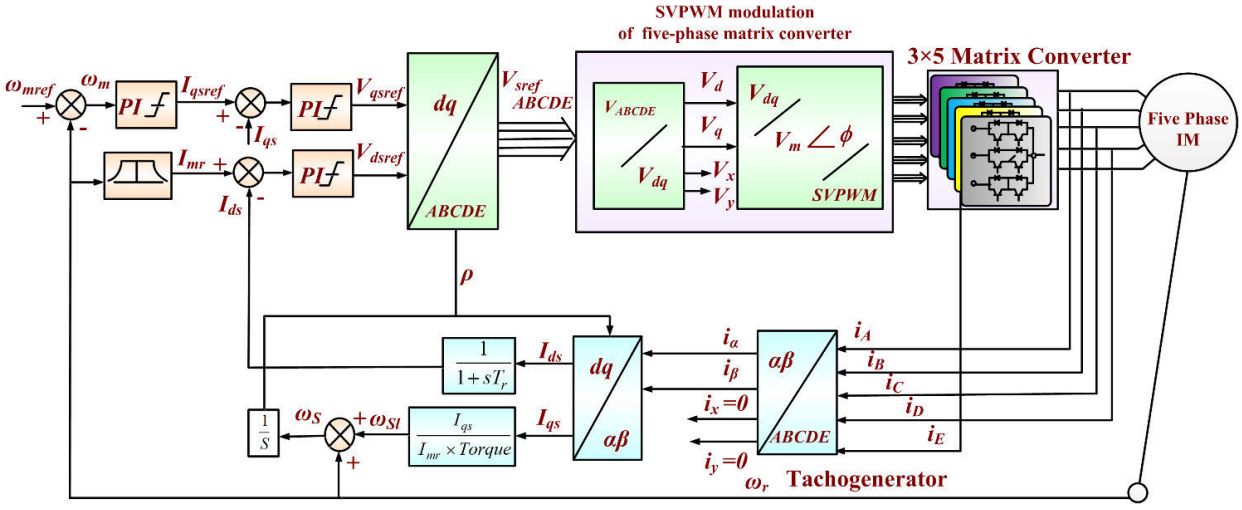

FIGURE 2. Field-oriented control scheme for five-phase IM based on SVPWM of MC.

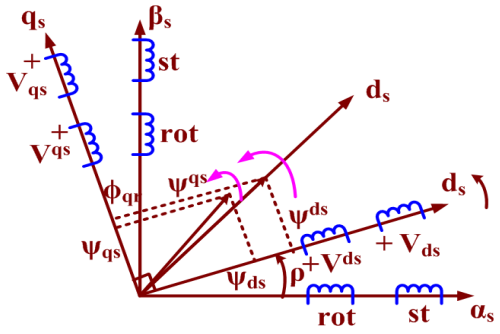

FIGURE 3. Machine stator and rotor representation in synchronously rotating reference frame.

$$\psi_{qs} = L_{ss} i_{qs} + L_m i^{qs} \tag{15}$$
$$\psi^{ds} = L'_{rr} i^{ds'} + L_m i_{ds} \tag{16}$$
$$\psi^{qs} = L'_{rr} i^{qs'} + L_m i_{qs} \tag{17}$$

From (14)-(17), one can derive (18) and (19). By putting (18)-(19) in (13) and the resulting set of equations can be written as (22), which is the description of the voltage subsystem in the induction machine.

$$i^{ds'} = \left(\psi^{ds} - L_m i_{ds}\right) \times \frac{1}{L'_{rr}} \tag{18}$$
$$i^{qs'} = \left(\psi^{qs} - L_m i_{qs}\right) \times \frac{1}{L'_{rr}} \tag{19}$$

In the same way, the expression for generated electromagnetic torque, written in (23). V^{ds} and V^{qs} for the rotor is zero as it is shorted.

$$V_{ds} = (r_s + L_{ss}p) i_{ds} - \omega_s L_{ss} i_{qs} + L_m p \left(\frac{\psi^{ds} - L_m i_{ds}}{L'_{rr}}\right) - L_m \omega_s \left(\frac{\psi^{qs} - L_m i_{qs}}{L'_{rr}}\right) \tag{20}$$

$$V_{ds} = (r_s + L_{ss}p - \frac{L_m^2}{L'_{rr}}p) i_{ds} - \omega_s (L_{ss} + \frac{L_m^2}{L'_{rr}}) i_{qs} + L_m p \frac{\psi^{ds}}{L'_{rr}} - L_m \omega_s \frac{\psi^{qs}}{L'_{rr}} \tag{21}$$

Suppose the d_s component is chosen along with the ψ^{ds} then $\psi^{qs} = 0$. The final equation (27) tells that the generated torque equals the multiplication of stator q-axis current and rotor flux, similar to the separately excited DC motor. Here the orientation is done along the rotor field vector.

$$\begin{bmatrix} V_{ds} \\ V_{qs} \\ V^{ds} \\ V^{qs} \end{bmatrix} = \begin{bmatrix} r_s + \sigma L_{ss} p & -\omega_s \sigma L_{ss} & \frac{L_m p}{L'_{rr}} & -\frac{L_m \omega_s}{L'_{rr}} \\ \omega_s \sigma L_{ss} & r_s + \sigma L_{ss} p & -\frac{L_m \omega_s}{L'_{rr}} & \frac{L_m p}{L'_{rr}} \\ -\frac{r_r L_m}{L'_{rr}} & 0 & \frac{r'_r}{L'_{rr}} + p & -\omega_s + \omega_{rr} \\ 0 & -\frac{r_r L_m}{L'_{rr}} & \omega_s - \omega_{rr} & \frac{r'_r}{L'_{rr}} + p \end{bmatrix} \times \begin{bmatrix} i_{ds} \\ i_{qs} \\ \psi^{ds} \\ \psi^{qs} \end{bmatrix} \tag{22}$$

$$T = \frac{L_m}{L'_{rr}} (i_{qs} \psi^{ds} - i_{ds} \psi^{qs}) \tag{23}$$
$$V^{qs} = 0 = \frac{r_r L_m}{L'_{rr}} i_{qs} + (\omega_s - \omega_{rr}) \psi^{ds} \tag{24}$$
$$V^{ds} = 0 = -\frac{r_r L_m}{L'_{rr}} i_{ds} + (\frac{r_r}{L'_{rr}} + p) \psi^{ds} \tag{25}$$
$$\psi^s = \psi^{ds} = \frac{r_r L_m}{L'_{rr}} * \frac{1}{s + \frac{r_r}{L'_{rr}}} I_{ds}(s) \tag{26}$$
$$T = \frac{L_m}{L'_{rr}} i_{qs} \psi^s \tag{27}$$

TABLE 2. Common switching vectors in different input currents and output voltage sectors of five-phase direct MC.

		I Sect		
		1 / 4	2 / 5	3 / 6
V Sect	1 / 6	±(1,3,13,15) ML	±(2,3,14,15) ML	±(1,2,13,14) ML
	2 / 7	±(1,3,4,6) ML	±(2,3,5,6) ML	±(1,2,4,5) ML
	3 / 8	±(4,6,7,9) ML	±(5,6,8,9) ML	±(4,5,7,8) ML
	4 / 9	±(7,9,10,12) ML	±(8,9,11,12) ML	±(7,8,10,11) ML
	5 / 10	±(10,12,13,15) ML	±(11,12,14,15) ML	±(10,11,13,14) ML

IV. MODULATION OF THREE-TO-FIVE PHASE DMC

In the direct MC, any output phase can be connected with any of the input phases. Fifteen bidirectional switches are there in an MC combination, encompassing a total 2^{15} switching possibilities. Out of these, only 93 switching arrangements are established to control the input current and output voltage [12]. The switching function considering the switching constraints $S_{ak} + S_{bk} + S_{ck} = 1$ is well-defined as: $S_{jk} = \{1, 0\}$ for closed and open switch, respectively. Here, j is input phase $\{a, b, c\}$ and k is output phase $\{A, B, C, D, E\}$. The objective of the SVPWM is to accomplish five-phase harmonic free output voltages and currents. The SVPWM algorithm is established on demonstrating the three input phase currents and five output line voltages on the space vector planes. There are six sectors of the input current and ten sectors of output voltage. The complete control of the MC is possible by governing the common vectors between input current and output voltage sectors [12]–[14]. These are 16 in number, forming large and second large (medium) length vectors. Table 2 presents these common vectors in the first sector of the input current and output voltage, where vectors of medium length and large length are ±1, ±13, ±3, ±15 M and ±1, ±13, ±3, ±15 L, respectively. Vectors are numbered sequentially, starting from the horizontal axis anticlockwise. "±" sign indicates two vectors separated by 180° in phases having the same magnitude. The output reference voltage has a projection of V' and V'' at two sides of the sector. At any fixed position, suppose $+1M$, there are three voltage vectors 0.25 V_{ab}, V_{bc}, and V_{ca}.

These have three different magnitudes at an instant. Among these, having the largest and medium magnitude is selected for the implementation. Selected vectors in the direction of V' and V'' must be of the same input phase connection. Therefore, these vectors +1M, −3M, −13M, +15M, and +1L, −3L, −13L, +15L are common in sector I. These vectors are presented in Fig. 4. Where, for the current first sector α_i vary from $-\pi/6$ to $+\pi/6$ and for voltage vector V_o varies from $-\pi/10$ to $+\pi/10$. The input current and output voltages can be presented in terms of space vectors as,

$$\vec{V}_i = \frac{2}{3}\left(V_{ab} + V_{bc}.e^{j\frac{2\pi}{3}} + V_{ca}.e^{j\frac{4\pi}{3}}\right) = V_i.e^{j\alpha_i} \quad (28)$$

$$\vec{I}_i = \frac{2}{3}\left(I_a + I_b.e^{j\frac{2\pi}{3}} + I_c.e^{j\frac{4\pi}{3}}\right) = I_i.e^{j\alpha_i} \quad (29)$$

$$\vec{V}_o = \frac{2}{5}\left(V_{AB} + V_{BC}.e^{j\frac{2\pi}{5}} + V_{CD}.e^{j\frac{4\pi}{5}} + V_{DE}.e^{j\frac{6\pi}{5}} + V_{EA}.e^{j\frac{8\pi}{5}}\right) = V_o.e^{j\alpha_O} \quad (30)$$

The maximum voltage transfer ratio can be obtained as 0.7886 times the input voltage. To achieve the power factor-controlled operation, let $\vec{V}_i$ be the input line voltage and $\vec{V}_o$ the desired output line voltage space vector instantly. The input phase $\vec{e}_i$ voltage vector is given by (31).

$$\vec{e}_i = \frac{1}{\sqrt{3}}\vec{V}_i.e^{-j\frac{\pi}{6}} \quad (31)$$

For input power factor control, the direction of the input current space vector $\vec{I}_i$ has to be controlled according to $\vec{e}_i$. For unity power factor operation, $\vec{I}_i$ and $\vec{e}_i$ should be in the same phase. Consider $\vec{I}_i$ and $\overline{V}_o$ are in sector 1, large and medium vector configurations comprising of $\overline{V}'_o$ are shown in Fig. 4. Similarly $\vec{I}_i$ is determined into components $\vec{I}'_i$ and $\vec{I}''_i$ along with the two adjoining vector directions. Possible switching to produce the resolved currents and voltages are,

$\vec{V}'_o$: $\pm 1L, \pm 2L, \pm 3L$ and $\pm$ 1M, $\pm$ 2M, $\pm$ 3M
$\vec{V}''_o$: $\pm 13L, \pm 14L, \pm 15L$ and $\pm$ 13M, $\pm$ 14M, $\pm$ 15M
$\vec{I}'_i$: $\pm 3L, \pm 6L, \pm 9L, \pm$ 12L, $\pm$ 15L and
$\pm 3M, \pm 6M, \pm 9M, \pm$ 12M, $\pm$ 15M
$\vec{I}''_i$: $\pm 1L, \pm 4L, \pm 7L, \pm$ 10L, $\pm$ 13L and
$\pm 1M, \pm 4M, \pm 7M, \pm$ 10M, $\pm$ 13M

Complete control is possible by controlling the common switching states of input current and output voltage components. The common switching states are,

$\pm 1L, \pm 3L, \pm 1M, \pm$ 3M and $\pm$ $13L, \pm 15L, \pm 13M, \pm$ 15M.

The sign "±" indicates the corresponding space vectors are in opposite directions. Out of these two switching vectors with opposite signs, only one is used at a time. For example, the duty cycle is calculated for switching states with positive signs; if it comes positive, then the switching vector corresponding to positive sign switching state is selected for reference modulation; otherwise, a space vector with a switching state with a negative sign is carefully chosen.

The desired $\vec{V}'_o$ can be estimated by applying two medium and two large switching patterns conforming to four space vectors $\vec{V}'_o$. Out of four possible switchings, two contribute

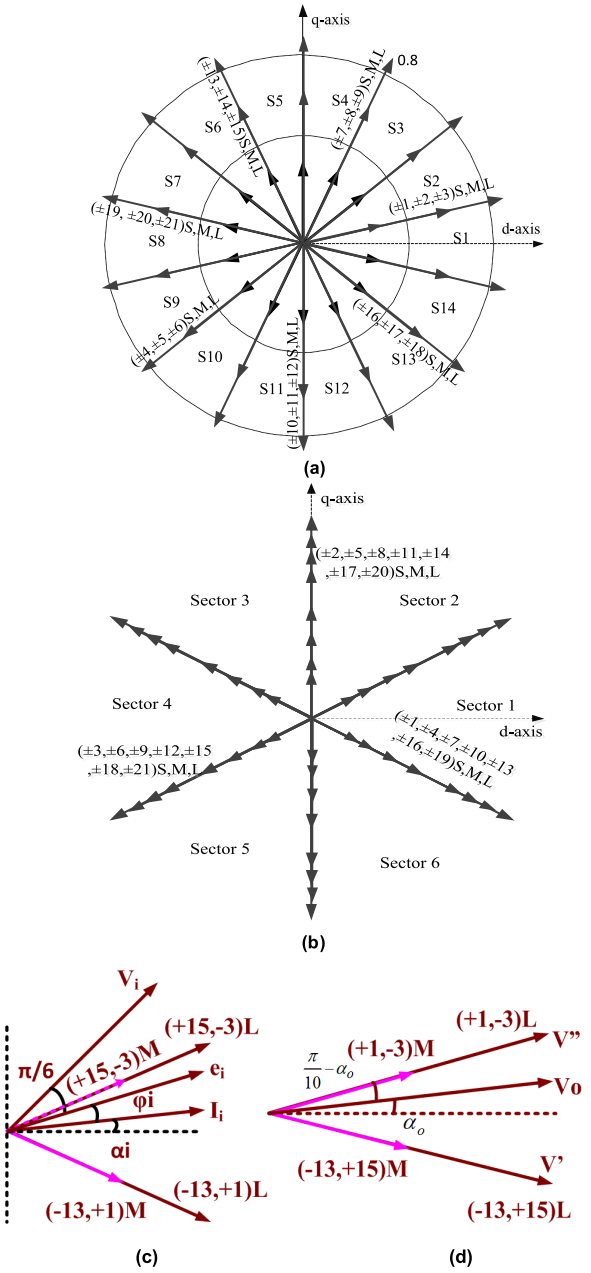

FIGURE 4. Space vectors diagram for three-phase to five-phase DMC (a) All active output voltages (b) input currents and for sector 1 (c) Input currents (d) output voltages space vectors.

the higher voltage values corresponding to large vectors. The reaming two arrange for the medium voltage meeting the requirements to medium vectors with the same sense of $\vec{V}_o'$ being chosen. Correspondingly, one zero and four different switching configurations define $\vec{V}_o''$.

Table 3, $\vec{V}_o'$ is obtained from the pattern $+1M$, $-3M$ for medium and $+1L$, $-3L$ for large vectors while for $\vec{V}_o''$ these are $+13M$, $-15M$ and $+13L$, $-15L$. These eight patterns determine the output voltage and input current.

Applying the SVPWM technique, the calculation of duty ratio'd' has been explained in detail [16]. It is obtained in (32) and (33), where the voltage transfer ratio is transferred.

TABLE 3. Switching sequence of output voltage vector in sector 1.

Vec. No.	Input a b, c	Output phases A	B	C	D	E	Output line voltage V_{AB}	V_{BC}	V_{CD}	V_{DE}	V_{EA}
0	b, b	b	b	b	b	b	0	0	0	0	0
+1 M	a, b	a	b	b	b	b	Vab	0	0	0	-Vab
-13 L	a, b	a	b	b	b	a	0	Vab	0	0	-Vab
+1 L	a, b	a	a	b	b	a	0	Vab	0	-Vab	0
-13 M	a, b	a	a	b	a	a	0	0	Vab	0	0
0	a, a	a	a	a	a	a	0	0	0	0	0
+15 M	a, c	a	a	c	a	a	0	0	-Vca	Vca	0
-3 L	a, c	a	a	c	c	a	0	-Vca	0	Vca	0
+15 L	a, c	a	c	c	c	a	0	-Vca	0	0	Vca
-3 M	a, c	a	c	c	c	c	-Vca	0	0	0	Vca
0	c, c	c	c	c	c	c	0	0	0	0	0

It is noteworthy that the obtained results are effective for $-\pi/10 \le \alpha_o \le \pi/10$ and $0 \le \alpha_i \le \pi/3$.

$$\begin{cases} d_{1L}^{+} = q.L.\dfrac{10}{3\sqrt{3}}\sin\left(\dfrac{\pi}{10}+\alpha_o\right).\sin\left(\dfrac{\pi}{3}-\alpha_i\right) \\ d_{3L}^{-} = q.L.\dfrac{10}{3\sqrt{3}}\sin\left(\dfrac{\pi}{10}+\alpha_o\right).\sin\left(\alpha_i\right) \\ d_{1M}^{+} = q.M.\dfrac{10}{3\sqrt{3}}\sin\left(\dfrac{\pi}{10}+\alpha_o\right).\sin\left(\dfrac{\pi}{3}-\alpha_i\right) \\ d_{3M}^{-} = q.M.\dfrac{10}{3\sqrt{3}}\sin\left(\dfrac{\pi}{10}+\alpha_o\right).\sin\left(\alpha_i\right) \end{cases} \tag{32}$$

Similarly for $\vec{V}_o''$,

$$\begin{cases} d_{13L}^{+} = q.L.\dfrac{10}{3\sqrt{3}}\sin\left(\dfrac{\pi}{10}-\alpha_o\right).\sin\left(\dfrac{\pi}{3}-\alpha_i\right) \\ d_{15L}^{-} = q.L.\dfrac{10}{3\sqrt{3}}\sin\left(\dfrac{\pi}{10}-\alpha_o\right).\sin\left(\alpha_i\right) \\ d_{13M}^{+} = q.M.\dfrac{10}{3\sqrt{3}}\sin\left(\dfrac{\pi}{10}-\alpha_o\right).\sin\left(\dfrac{\pi}{3}-\alpha_i\right) \\ d_{15M}^{-} = q.M.\dfrac{10}{3\sqrt{3}}\sin\left(\dfrac{\pi}{10}-\alpha_o\right).\sin\left(\alpha_i\right) \end{cases} \tag{33}$$

Similarly, the obligatory switchings and their duty ratio of can be calculated. The sum of the proportions must be less than unity.

$$d_{1L}^{+} + d_{3L}^{-} + d_{13L}^{+} + d_{15L}^{-} + d_{1M}^{+} + d_{3M}^{-} + d_{13M}^{+} + d_{15M}^{-} \le 1 \tag{34}$$

V. RESULTS AND DISCUSSION

The induction motor parameters are tabulated in Table 4. The proposed FOC scheme is simulated and verified on a 2-hp five-phase IM. The three-to-five phase MC is used as a source of voltage for the induction motor. The developed model is tested for different set speeds. Moreover, the disturbance is also used externally by applying load torques in a stepped manner, and the system's response is noted and analyzed. Supply voltage 230V is given to the matrix converter, and

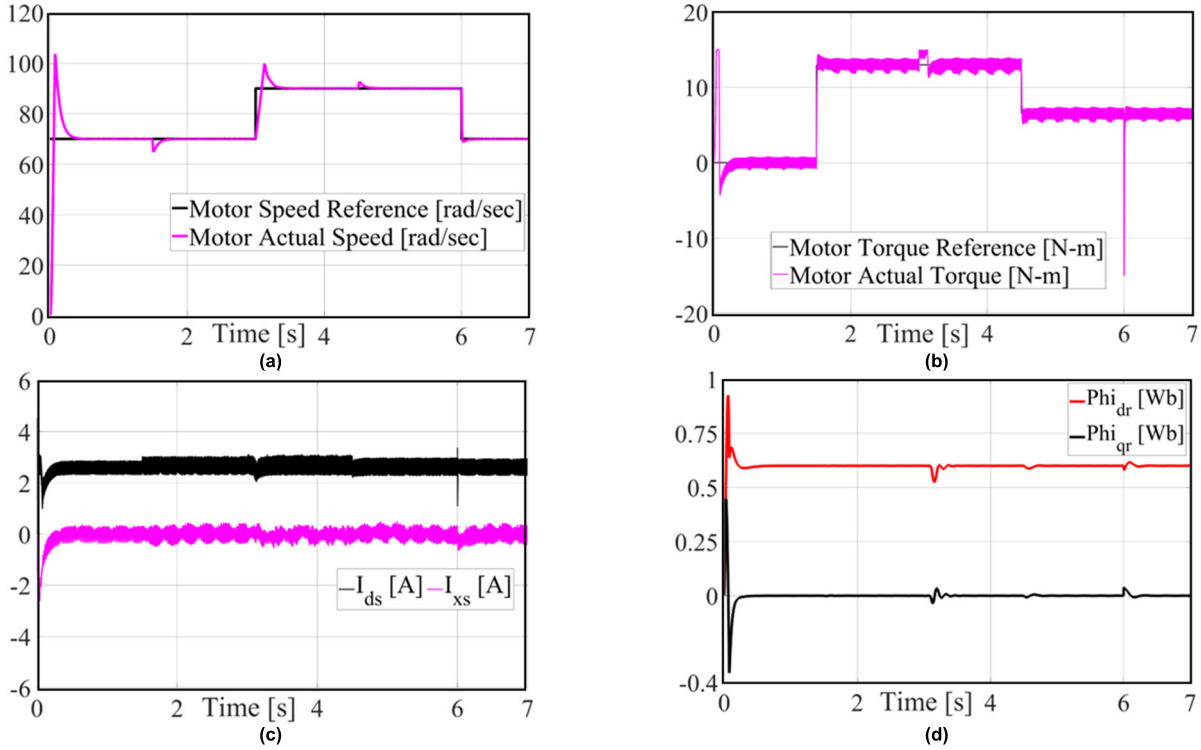

FIGURE 5. Simulation results (a) Speed response of the controlled drive system, (b) torque response of the controlled drive system, (c) Stator current, (d) Rotor flux of the five-phase induction motor.

TABLE 4. Simulation parameters.

Parameter	value
P	2 HP
V_s (V)	230
Pole pairs	2
R_r, R_s (Ω)	6.4,7.2
L_s (mH)	103.1
L_r (mH)	92.2
ω_r (rad)	157
L_m (H)	1.013
J_m (kgm^2)	0.021

the model system's response and the control algorithm are observed.

The sequence of the load torque and the speed reference application is given as,

a) The speed reference at t = 0 sec is 130 rad/sec

b) The load torque of 10 N-m is applied at t = 1.5 sec,

c) At t = 3 sec, the speed reference is increased from 130 to 150 rad/sec

d) At t = 4.5 sec, the load torque is reduced from 10 N-m to 6 N-m and

e) At t = 6 sec, the speed reference is reduced to 120 rad/sec.

The rotor speed and resultant torque response of five-phase IM are shown in Fig 5(a)-(b), respectively. At first, the machine gradually rises to meet the requisite steady-state speed. Once the speed reaches its steady-state value, a load torque of 13 N-m is applied. Momentarily, a speed dip is observed at the load application. The control process helps to reinstate the speed to the reference value. The reference speed is increased at t = 3 sec. From Fig. 5, it is shown that the rotor speed tracks the reference speed, and corresponding more torque is required. That is observed in Fig. 5(b).

Further, it is observed that the drive tracks the reference speed at all the points in different speed and torque changing conditions. The actual speed of the rotor tracks the reference speed, thus displaying the dynamic behavior of the scheme.

At different loading conditions, stator current i_{ds} momentarily change; however, it restores its previous steady-state value.

The drive's control is confirmed by restoring the stator current and rotor flux in Fig. 5(c) and Fig. 5(d) at different torque and speed conditions. It can be observed that there is no demagnetization of flux, and the actual rotor speed follows the reference speed.

The stator phase 'A' current of five-phase IM at different loading conditions is shown in Fig. 6(a). At time 4.5 seconds, the load torque is changed from 13 N-m to 6.5 N-m at 90 rad/sec. It confirms the low current required to maintain the drive at the same speed. The locus of the five-phase stator current of $\alpha\beta$ and xy components is shown in Fig. 6(b). It is found that the five-phase current is balanced and sinusoidal since the xy component is insignificant. The output voltage of

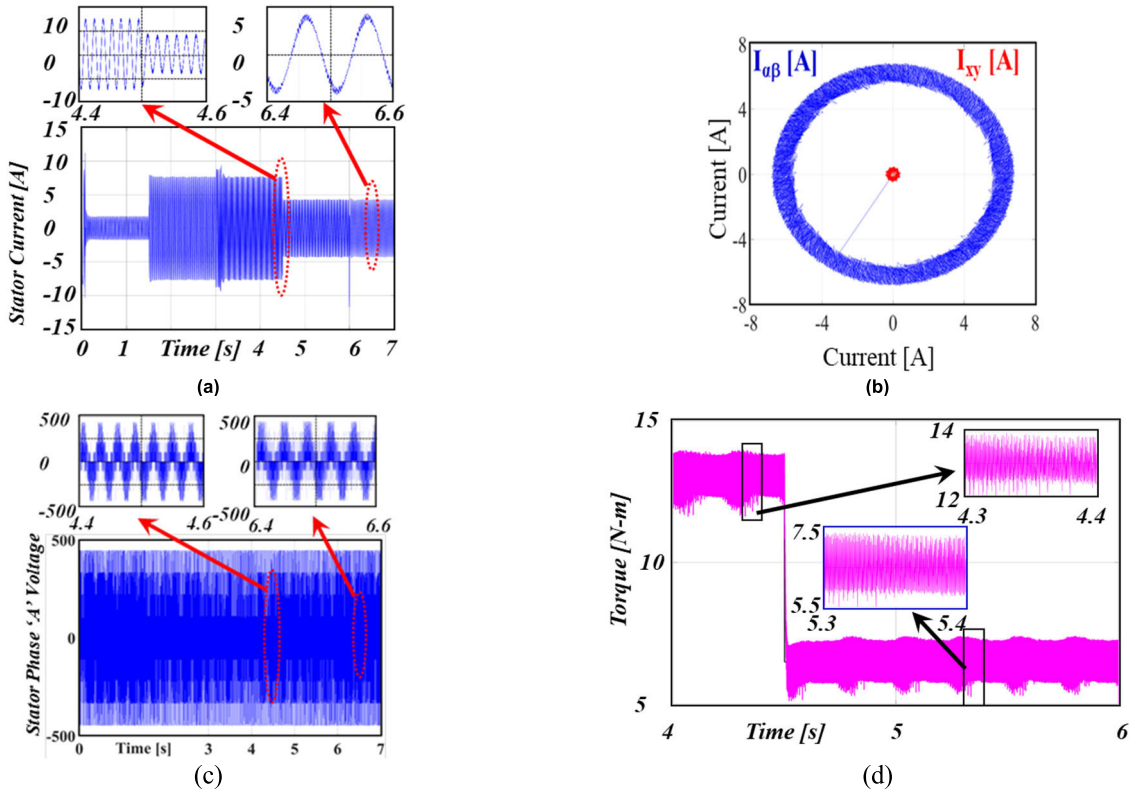

FIGURE 6. Simulation results (a) Stator phase 'A' current, (b) Locus of stator currents $\alpha\beta$ and xy components at 120-r/sec of rotor speed, (c) Stator phase 'A' voltage, (d) Torque ripple of the five-phase IM at different load conditions.

the three-to-five phase matrix converter for the control drive at different operating conditions is shown in Fig. 6(c) for the load change from 13 N-m to 6.5 N-m, and Fig. 6(d) is for steady-state operation at 70 rad/sec speed at 6.5 N-m torque.

The FPIM is changed from 90 rad/sec to 30% of synchronous speed at rated load torque to demonstrate robustness and accuracy of speed tracking performance. The response of the system is shown in Fig. 7.

In the FOC of five-phase IM, the reference torque and flux calculate the stator current i_{ds} and i_{qs}. To get the controlled operation of the drive, i_{ds} should remain controlled irrespective of the loading conditions of the drives. Fig 5(c) shows the stator current direct axis component i_{ds} and the loss component i_{xs}, corresponding to the speed and torque.

To reach the desired speed within minimum time, maximum torque is applied on the motor resulting in fast acceleration. However, the torque decreases when the motor gets near the desired speed, and steady tracking is observed within 0.5 seconds.

When the speed reference is reduced, maximum negative torque is applied to achieve fast deceleration. An undershoot is observed in the FPIM response before settling at 30% of synchronous speed.

Harmonic spectrum of motor torque (at rated load torque of 10Nm) at switching frequencies of 4 kHz, 2 kHz, and 1 kHz are shown in Fig. 8(a) – Fig. 8(c), respectively. Here, all low-frequency components (<10 * fundamental frequency) are

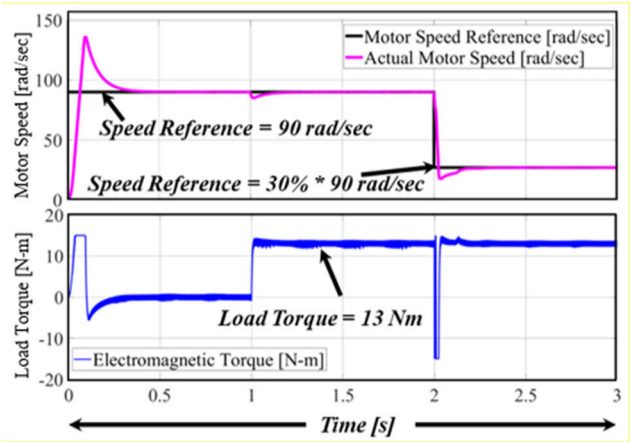

FIGURE 7. Tracking the performance of five-phase induction motor from 100% to 20% of rated speed at rated torque.

eliminated due to the PWM operation of the matrix converter. Conclusively, the process at a higher switching frequency results in low THD content. However, a higher switching frequency operation leads to higher switching losses in the converter (which requires more oversized heat sinks). Thus, the selection of switching frequency plays a crucial role in motor drive performance, and it must be selected depending upon the desired requirements of size, cost, and performance reliability.

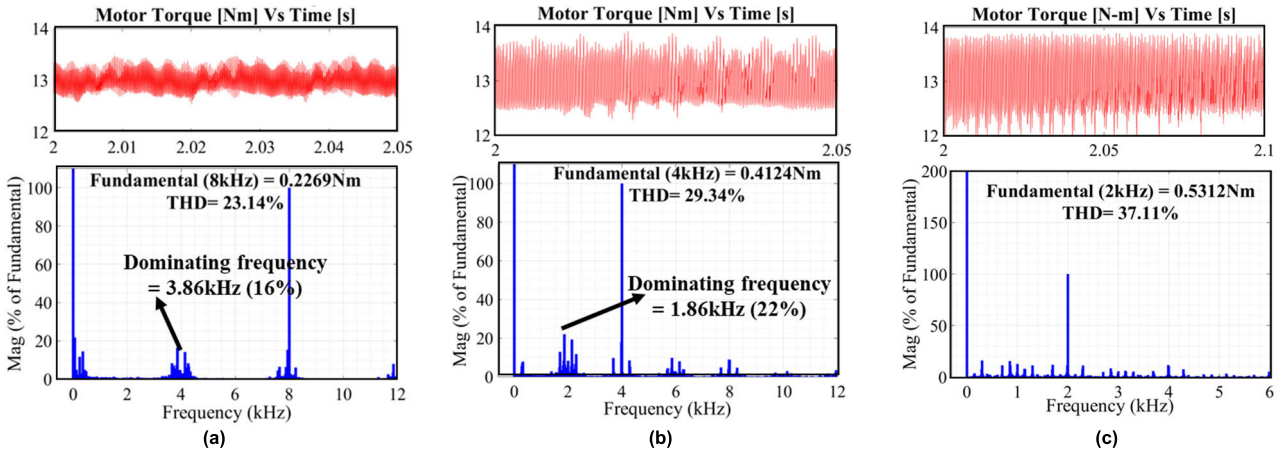

FIGURE 8. Harmonic spectrum of motor torque ripple for (a) 4kHz (b) 2kHz, and (c) 1kHz switching frequency.

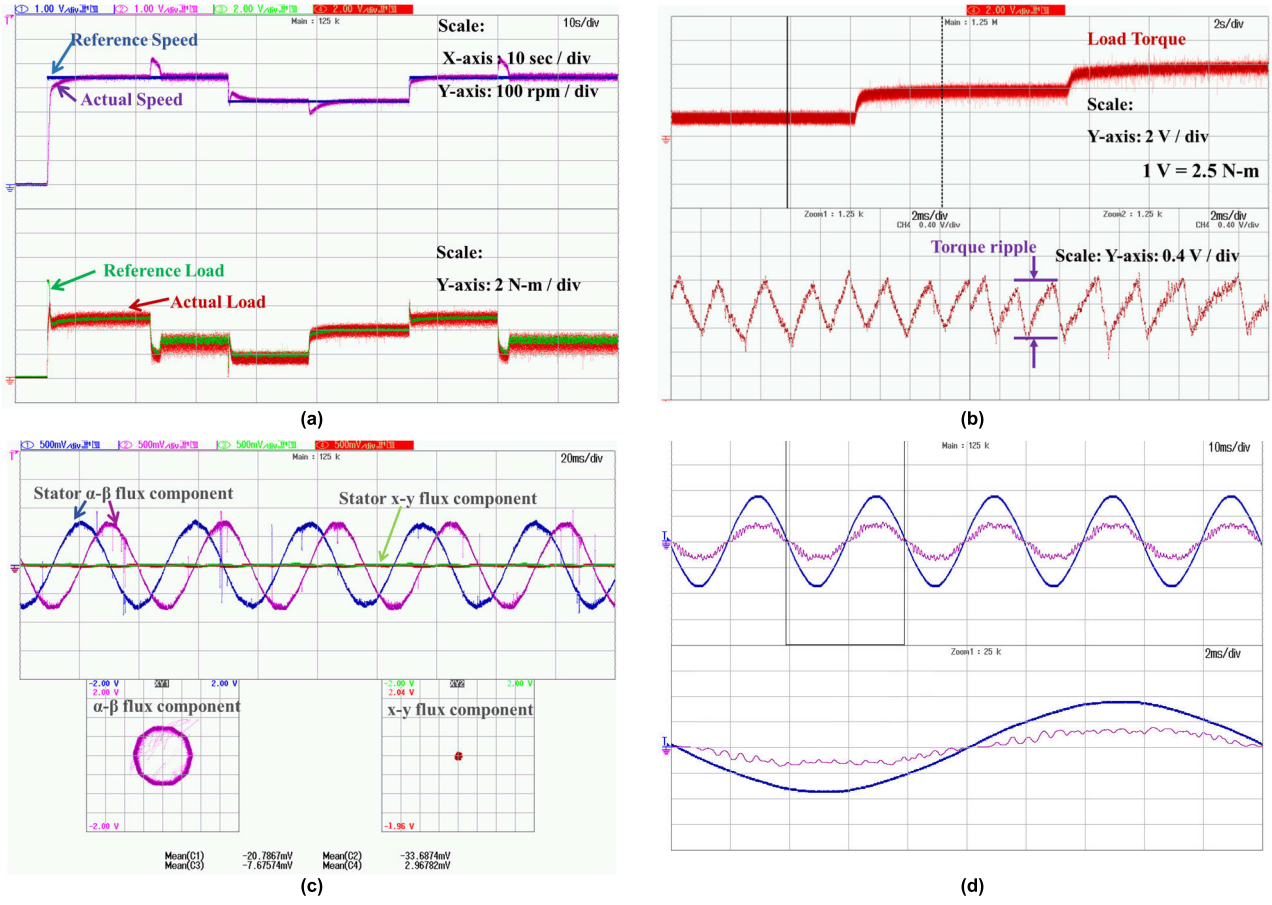

FIGURE 9. Experimental results (a) Speed and torque response of three-to-five phase MC fed five-phase IM, (b) Torque ripple of FPIM at different load conditions, (c) Stator $\alpha\beta$ and xy flux response of the motor under load condition. (d) Input phase voltage and current to show unity power factor control [X-axis: 10ms/div, Y-axis: 2.0 A/div, and 200.0 V/div].

The existence of torque ripple leads to vibration issues that can hamper the life of the motor drive. Conventionally, low-frequency torque ripples are more damaging than high-frequency torque ripples easily filtered out by the motor inertia.

The proposed scheme is also validated through the experiments. A 2 kW five-phase IM with a rated torque of 15 N-m and six poles is used for testing purposes. The control algorithm is implemented using the dSPACE 1006 board, giving the user to program at the FPGA level. For feedback of current

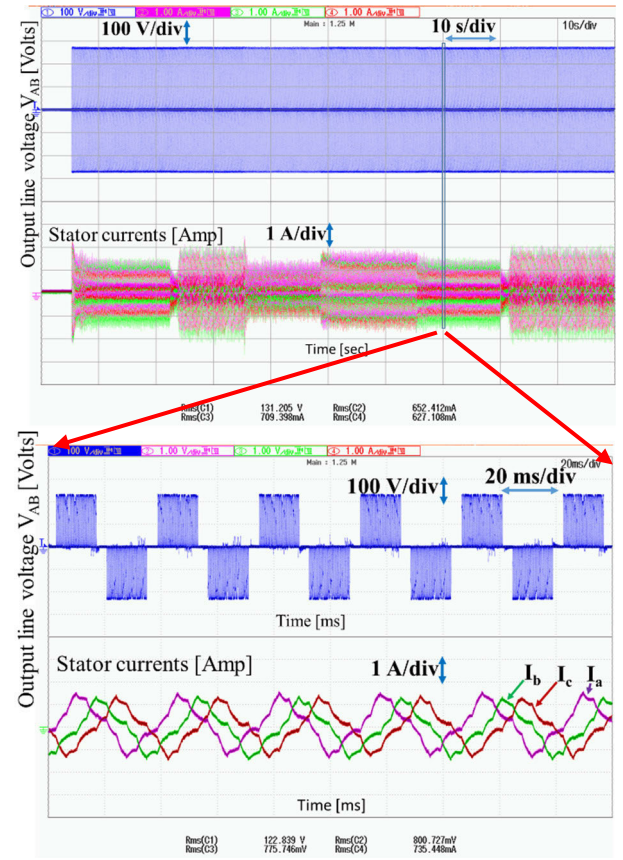

(a)

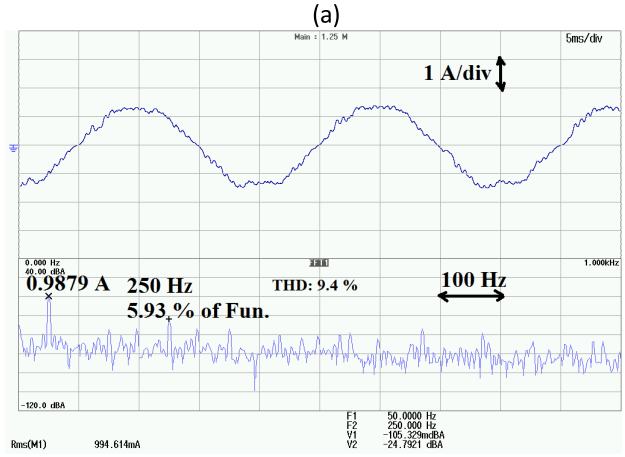

(b)

FIGURE 10. **Experimental results (a) The line voltage and stator current and their zoomed waveform at different transitions of speed and load torque. (b) Input current spectrum of matrix converter.**

and voltage into the dSPACE, LEM 55A and LEM 25P are used. For loading of five-phase IM, a separately excited DC generator is employed, which indirectly loads the IM through electrical loads connected at the terminal of the generator. For a sampling of flux and torque, the sample time Ts = 90μs is used. The switching frequency is fixed at 2 kHz. The speed of 500 RPM and respective torque is given with a load of 5 N-m, and the motor's actual speed also reaches the reference speed. Then at time t = 22 s load of the motor is reduced from 5 N-m to 2.5 N-m, the motor's actual speed retracts to the reference speed after some initial deviation.

Responses are shown in Fig. 9(a). At t = 5 s reference speed reaches the desired speed within minimum time, maximum torque is applied on the motor resulting in fast acceleration.

However, the torque decreases when the motor gets near the desired speed, and steady tracking is observed within 0.5 seconds. When the speed reference is reduced, maximum negative torque is applied to achieve fast deceleration. An undershoot is observed in the FPIM response before settling at 30% of synchronous speed. The existence of torque ripple leads to vibration issues that can hamper the life of the motor drive. Conventionally, low-frequency torque ripples are more damaging than high-frequency torque ripples easily filtered out by the motor inertia.

At t = 35 s, the reference speed is reduced from 500 RPM to 400 RPM keeping the constant electrical load to the motor's overloading as the speed decreases. Similarly, the motor's actual speed follows the reference speed for the transition states marked in Fig. 9(a). The torque ripple of the motor is shown in Fig. 9(b) for different load conditions. The torque ripple is about 0.9 volts, whereas the rated torque is 15 N-m, i.e., 6 volts. Thus the torque ripple is around 15% of the rated torque. The xy flux trajectory is shown in Fig. 9(c), and it is observed that the maximum magnitude of xy flux is almost negligible compared to the rated flux. The xy flux is eliminated because of the volt-second balance technique applied in the modulation of the converters. The actual current tracks the desired value without delay. The unity power factor of the matrix converter is confirmed from the Fig. 9(d) shows input voltage and current, ensuring almost zero phase delay.

Moreover, the stator currents and line voltage have been included in the experimental results. The dynamics of stator currents have been presented when the reference speed is changed. Fig. 10 shows the corresponding output line voltage V_{AB}, and stator currents with its zoomed waveform for five-phase induction motor at the transition states of speed and torque. Apart from that, the spectrum of the input current of the matrix converter is presented. The THD of matrix converter input current is 9.4% at 0.8 modulation index.

VI. CONCLUSION

The field-oriented control of a five-phase induction motor is performed. The drive is fed from an SVPWM controlled three-to-five phase DMC. The analytical results are verified using simulation and experiments. The modulation of three-to-five phase DMC is achieved with minimum possible switchings. There are at least ten switching transitions during a switching cycle. The xy component of flux is eliminated, reducing the spoiling of stator current distortion and improving the reliability. Applying the volt-second principle in the modulation of space vectors of the matrix converter eliminates the xy flux component. The dynamic characteristics of the motor is confirmed for different load torque and speed conditions. The matrix converter control achieved the

input side current in phase with the input voltage and better dynamic performance of the FPIM with low torque ripple and almost zero xy flux.

ACKNOWLEDGMENT

This publication was made possible by NPRP Grant from the Qatar National Research Fund under project grant NPRP-4-152-2-053. The statements made herein are solely the responsibility of the authors. This work was also supported in part by the Taif University Researchers Supporting Project, Taif University, Taif, Saudi Arabia, under Grant TURSP-2020/278, and in part by the Collaborative Research Grant Scheme (CRGS) Project under grants CRGS/Mohd Tariq/01 and CRGS/Mohd Tariq/02, Hardware-In-the-Loop (HIL) Laboratory, Department of Electrical Engineering, Aligarh Muslim University, India.

REFERENCES

[1] K. N. Pavithran, R. Parimelalagan, and M. R. Krishnamurthy, "Studies on inverter-fed five-phase induction motor drive," *IEEE Trans. Power Electron.*, vol. PEL-3, no. 2, pp. 224–235, Apr. 1988.

[2] H. Xu, H. A. Toliyat, and L. J. Petersen, "Five-phase induction motor drives with DSP-based control system," *IEEE Trans. Power Electron.*, vol. 17, no. 4, pp. 524–533, Jul. 2002.

[3] E. Levi, R. Bojoi, F. Profumo, H. A. Toliyat, and S. Williamson, "Multi-phase induction motor drives—A technology status review," *IET Electr. Power Appl.*, vol. 1, no. 4, pp. 489–516, Jul. 2007.

[4] E. Levi, "Multiphase electric machines for variable-speed applications," *IEEE Trans. Ind. Electron.*, vol. 55, no. 5, pp. 1893–1909, May 2008.

[5] D. Dujic, M. Jones, and E. Levi, "Continuous carrier-based vs. space vector PWM for five-phase VSI," in *Proc. Int. Conf. Comput. Tool (EUROCON)*, Warsaw, Poland, Sep. 2007, pp. 1772–1779.

[6] P. S. N. de Silva, "Development of space vector modulation strategies for five phase voltage source inverters," in *Proc. 2nd IEE Int. Conf. Power Electron., Mach. Drives*, Edinburgh, U.K., Mar. 2004, pp. 650–655.

[7] A. Iqbal and E. Levi, "Space vector modulation schemes for a five-phase voltage source inverter," in *Proc. Eur. Conf. Power Electron. Appl.*, Dresden, Germany, Sep. 2005, p. 12.

[8] K. B. Tawfiq, M. N. Ibrahim, E. E. EL-Kholy, and P. Sergeant, "Comparative analysis of refurbishing methods of three-phase synchronous reluctance machines to five-phase with minimum cost," *IEEE Trans. Ind. Appl.*, vol. 57, no. 6, pp. 6007–6022, Nov. 2021, doi: 10.1109/TIA.2021.3117485.

[9] A. Trentin, L. Empringham, L. de Lillo, P. Zanchetta, P. Wheeler, and J. Clare, "Experimental efficiency comparison between a direct matrix converter and an indirect matrix converter using both Si IGBTs and SiC MOSFETs," *IEEE Trans. Ind. Appl.*, vol. 52, no. 5, pp. 4135–4145, Sep. 2016.

[10] M. Venturini and A. Alesina, "The generalised transformer: A new bidirectional, sinusoidal waveform frequency converter with continuously adjustable input power factor," in *Proc. IEEE Power Electron. Spec. Conf.*, Jun. 1980, pp. 242–252.

[11] M. Jussila and H. Tuusa, "Comparison of direct and indirect matrix converters in induction motor drive," in *Proc. 32nd Annu. Conf. IEEE Ind. Electron. (IECON)*, Paris, France, Nov. 2006, pp. 1621–1626.

[12] A. Iqbal, S. M. Ahmed, and H. Abu-Rub, "Space vector PWM technique for a three-to-five-phase matrix converter," *IEEE Trans. Ind. Appl.*, vol. 48, no. 2, pp. 697–707, Apr. 2012.

[13] K. Rahman, A. Iqbal, and R. Al-ammari, "Space vector model of a three-phase to five-phase AC/AC converter," in *Proc. Africon*, Sep. 2013, pp. 1–6.

[14] J. Szczepanik, "Multi-phase matrix converter for power system application," in *Proc. IEEE Int. Symp. Ind. Electron.*, Oct. 2014, pp. 2625–2630.

[15] K. Rahman, A. Iqbal, A. A. Abduallah, R. Al-ammari, and H. Abu-Rub, "Space vector pulse width modulation scheme for three to seven phase direct matrix converter," in *Proc. IEEE Appl. Power Electron. Conf. Expo. (APEC)*, Mar. 2014, pp. 595–601.

[16] S. Payami and R. K. Behera, "An improved DTC technique for low-speed operation of a five-phase induction motor," *IEEE Trans. Ind. Electron.*, vol. 64, no. 5, pp. 3513–3523, May 2017.

[17] B. Chikondra, U. R. Muduli, and R. K. Behera, "An improved open-phase fault-tolerant DTC technique for five-phase induction motor drive based on virtual vectors assessment," *IEEE Trans. Ind. Electron.*, vol. 68, no. 6, pp. 4598–4609, Jun. 2021.

[18] U. R. Muduli, B. Chikondra, and R. K. Behera, "Space vector PWM based DTC scheme with reduced common mode voltage for five-phase induction motor drive," *IEEE Trans. Power Electron.*, vol. 37, no. 1, pp. 114–124, Jan. 2022, doi: 10.1109/TPEL.2021.3092259.

[19] K. Kubota and K. Matsuse, "Speed sensorless field-oriented control of induction motor with rotor resistance adaptation," *IEEE Trans. Ind. Appl.*, vol. 30, no. 5, pp. 1219–1224, Sep. 1994.

[20] K. Wang, Y. Li, Q. Ge, and L. Shi, "An improved indirect field-oriented control scheme for linear induction motor traction drives," *IEEE Trans. Ind. Electron.*, vol. 65, no. 12, pp. 9928–9937, Dec. 2018.

[21] Z. Liu, Z. Zheng, Q. Wang, and Y. Li, "Enhanced rotor field-oriented control of multiphase induction machines based on symmetrical components theory," *IET Power Electron.*, vol. 12, no. 4, pp. 656–666, Apr. 2019.

[22] S. Khadar, H. Abu-Rub, and A. Kouzou, "Sensorless field-oriented control for open-end winding five-phase induction motor with parameters estimation," *IEEE Open J. Ind. Electron. Soc.*, vol. 2, pp. 266–279, 2021.

[23] U. R. Muduli, B. Chikondra, and R. K. Behera, "Direct torque control of 3×5 matrix converter fed five-phase IM drive using virtual vector concept," in *Proc. IEEE Appl. Power Electron. Conf. Expo. (APEC)*, Phoenix, AZ, USA, Jun. 2021, pp. 765–770, doi: 10.1109/APEC42165.2021.9487140.

[24] U. R. Muduli, B. Chikondra, and R. K. Behera, "Novel model predictive DTC for Three-to-Five phase direct matrix converter fed induction motor drive," in *Proc. IEEE 12th Energy Convers. Congr. Expos. (ECCE-Asia)*, Singapore, May 2021, pp. 1505–1510, doi: 10.1109/ECCE-Asia49820.2021.9479067.

[25] D. Casadei, G. Serra, and A. Tani, "The use of matrix converters indirect torque control of induction machines," *IEEE Trans. Ind. Electron.*, vol. 48, no. 6, pp. 1057–1064, Dec. 2001.

[26] O. Ellabban, H. Abu-Rub, and B. Ge, "A quasi-Z-source direct matrix converter feeding a vector controlled induction motor drive," *IEEE J. Emerg. Sel. Topics Power Electron.*, vol. 3, no. 2, pp. 339–348, Mar. 2015.

[27] J. Zhang, H. Yang, T. Wang, L. Li, D. G. Dorrell, and D. D. Lu, "Field-oriented control based on hysteresis band current controller for a permanent magnet synchronous motor driven by a direct matrix converter," *IET Power Electron.*, vol. 11, no. 7, pp. 1277–1285, Jun. 2018.

[28] M. Pande, H. Jin, and G. Joos, "Modulated integral control technique for compensating switch delays and nonideal DC buses in voltage-source inverters," *IEEE Trans. Ind. Electron.*, vol. 44, no. 2, pp. 182–190, Apr. 1997.

[29] B. W. M. Narimani, "Two-level voltage source inverter," in *High-Power Converters AC Drives*. Hoboken, NJ, USA: Wiley, 2017, pp. 93–117, doi: 10.1002/9781119156079.ch6.

[30] L. Zheng, J. E. Fletcher, B. W. Williams, and X. He, "A novel direct torque control scheme for a sensorless five-phase induction motor drive," *IEEE Trans. Ind. Electron.*, vol. 58, no. 2, pp. 503–513, Feb. 2011.

[31] Y. N. Tatte and M. V. Aware, "Torque ripple and harmonic current reduction in a three-level inverter-fed direct-torque-controlled five-phase induction motor," *IEEE Trans. Ind. Electron.*, vol. 64, no. 7, pp. 5265–5275, Jul. 2017.

[32] R. Karampuri, J. Prieto, F. Barrero, and S. Jain, "A comparison between FOC and DTC methods for five-phase induction motor drives," in *Proc. Conf. 11th Int. Conf. Modeling Simul. Elect. Mach., Converters Syst.*, Valencia, Spain, May 2014.

KHALIQUR RAHMAN received the B.Tech. and M.Tech. degrees from Aligarh Muslim University (AMU), Aligarh, India, in 2008 and 2010, respectively, and the Ph.D. degree from Qatar University, Qatar, in 2019. From July 2010 to June 2012, he was a Lecturer with the Faculty of Electrical Engineering, AMU, where he is currently an Assistant Professor with the Electrical Engineering Department. His research interests include power electronics converters and drives, and renewable energy resources.

SYED RAHMAN (Student Member, IEEE) received the B.E. degree (Hons.) in electrical and electronics engineering from Osmania University, India, in 2012, and the M.Tech. degree in machine drives and power electronics from IIT Kharagpur, India, in 2014. He is currently pursuing the Ph.D. degree in electrical engineering with Texas A&M University, USA. He worked as a Research and Development Design Engineer with GE Healthcare, India, from October 2014 to January 2016. From February 2016 to December 2019, he was working as a Research Associate with Qatar University. He has published more than 20 refereed journal articles in power electronics and renewable energy integration. He was a recipient of the Thomas W. Powell '62 and Powell Industries Inc. Fellowship in 2021.

MAHAJAN SAGAR BHASKAR (Senior Member, IEEE) received the bachelor's degree in electronics and telecommunication engineering from the University of Mumbai, Mumbai, India, in 2011, the master's degree in power electronics and drives from the Vellore Institute of Technology, VIT University, India, in 2014, and the Ph.D. degree in electrical and electronic engineering from the University of Johannesburg, South Africa, in 2019. He worked as a Research Assistant with the Department of Electrical Engineering, Qatar University, Doha, Qatar, from 2018 to 2019. He is currently with the Renewable Energy Laboratory, Department of Communications and Networks Engineering, College of Engineering, Prince Sultan University, Riyadh, Saudi Arabia. He has published scientific articles in the field of power electronics, with particular reference to XY converter family, multilevel dc/dc and dc/ac converter, and high gain converter. He has authored more than 100 scientific articles. He is a member of the IEEE Industrial Electronics Society, the IEEE Power Electronics Society, the IEEE Industrial Application Society, the IEEE Power and Energy Society, the IEEE Robotics and Automation Society, the IEEE Vehicular Technology Society, the IEEE Young Professionals, and various IEEE councils and technical communities. He has received the Best Paper Research Paper Award from IEEE-CENCON 2019, IEEE-ICCPCT 2014, IET-CEAT 2016, and ETAEERE 2016, and sponsored lecture note in electrical engineering and Springer book series.

ATIF IQBAL (Senior Member, IEEE) received the B.Sc. (Hons.) and M.Sc. degrees in engineering (power system and drives) from Aligarh Muslim University (AMU), Aligarh, India, in 1991 and 1996, respectively, and the Ph.D. degree from Liverpool John Moores University, Liverpool, U.K., in 2006. He is currently an Associate Professor in electrical engineering with Qatar University, Qatar. He has been a Lecturer with the Department of Electrical Engineering, AMU, since 1991, where he served as a Full Professor until August 2016. He has authored/coauthored more than 300 research articles, one book, and three book chapters. His principal research interests include power electronics, multi-phase motor drives, and renewable energy sources. He became a fellow of IET (U.K.) in 2018 and IE (India) in 2012, and a Senior Member of IEEE in 2011. He has received the Best Research Papers Award at IEEE ICIT-2013, IET-SESICON-2013, and SIGMA 2018.

AMITH KHANDAKAR (Senior Member, IEEE) received the B.Sc. degree in electronics and telecommunication engineering from North South University, Bangladesh, and the master's degree in computing (networking concentration) from Qatar University. He is currently pursuing the Ph.D. degree with the Electrical and Computer Engineering Department, University of British Columbia. He graduated as the Valedictorian (President Gold Medal Recipient) of North South University. He is also a certified Project Management Professional and the Cisco Certified Network Administrator. Since the past ten years, he has been a Teaching Assistant and a Laboratory Instructor with the Electrical Engineering Department, Qatar University. After graduation, he was a consultant with a reputed insurance company in Qatar and a private company, which is a sub-contractor to National Telecom Service Provider in Qatar.

MOHD TARIQ (Senior Member, IEEE) received the bachelor's degree in electrical engineering from Aligarh Muslim University, Aligarh, the master's degree in machine drives and power electronics from IIT Kharagpur, and the Ph.D. degree in electrical engineering with a focus on power electronics and control from Nanyang Technological University (NTU), Singapore.

He is currently working as an Assistant Professor with Aligarh Muslim University, where he is directing various international and national sponsored research projects and leading a team of multiple researchers in the domain of power converters, energy storage devices, and their optimal control for electrified transportation and renewable energy application. Previously, he has worked as a Researcher with the Rolls-Royce@NTU Corporate Laboratory, Singapore, where he has worked on the design and development of power converters for more electric aircraft. Before joining his Ph.D., he has worked as a Scientist with the National Institute of Ocean Technology, Chennai, under the Ministry of Earth Sciences, Government of India, where he has worked on the design and development of BLDC motors for the underwater remotely operated vehicle application. He also served as an Assistant Professor with the Maulana Azad National Institute of Technology (MANIT), Bhopal, India. He has authored more than 150 research papers in international journals/conferences, including many articles in IEEE TRANSACTIONS/journals. He is also the inventor of approximately 25 patents granted/published by the patent offices of USA, Australia, U.K., EP, India, and China.

He was a recipient of the 2019 Premium Award for Best Paper in *IET Electrical Systems in Transportation* Journal for his work on more electric aircraft; the Best Paper Award from the IEEE Industry Applications Society's (IAS) and the Industrial Electronic Society (IES), Malaysia Section—Annual Symposium (ISCAIE-2016), Penang, Malaysia; and many other best paper awards in different international conferences. He was the Young Scientist Scheme Awardee supported by the Department of Science and Technology, Government of India, in 2019; the Young Engineer Awardee by the Institution of Engineers, India, in 2020; and the Young Research Awardee by AMU in 2021. He is also the Founder Chair of IEEE AMU Student Branch and IEEE SIGHT AMU.

BASEM ALAMRI (Member, IEEE) received the B.Sc. degree (Hons.) in electrical engineering from the King Fahd University of Petroleum and Minerals (KFUPM), in 2001, the M.Sc. degree in sustainable electrical power from Brunel University, London, U.K., in 2007, the M.Sc. degree (Hons.) in electrical power systems from King Abdulaziz University, Jeddah, Saudi Arabia, in 2008, and the Ph.D. degree in electrical power engineering from Brunel University, in 2017. He is currently an Assistant Professor of electrical engineering with the College of Engineering, Taif University. His research interests include power systems, power quality, power filter design, and smart grids, with a particular emphasis on the integration of renewable energy sources with power grids. He is a member of many international and local professional organizations. He is also a Certified Energy Auditor (CEA®), the Certified Energy Manager (CEM®), and the Certified Measurement and Verification Professional (CMVP®) of the Association of Energy Engineers (AEE), USA. He has received many awards and prizes, including a certificate from Advance Electronics Company (AEC) in recognition of the Outstanding Academic Achievement during the B.Sc. degree with KFUPM. He also received the National Grid (NG) Prize, the Power Grid Operator in U.K., for being the Top Distinction Student of the M.Sc. degree of the SEP Program with Brunel.